

## AERODYNAMIC DESIGN ANALYSIS OF MISSILES WITH STRAKE CONFIGURATIONS AT SUPERSONIC MACH NUMBERS

Engin Usta<sup>1</sup> and Kivanç Arslan<sup>2</sup>  
ROKETSAN Missile Industries Inc.  
Ankara, Turkey

İsmail H. Tuncer<sup>3</sup>  
Middle East Technical University  
Ankara, Turkey

### ABSTRACT

*Aerodynamics of missiles with very low aspect ratio fins are generally difficult to predict by using engineering level aerodynamics tools since linear theories break due to complex nature of the flow adjacent to the mutual interference of the body and fin. For this reason fast prediction methods are not very successful in most of the cases that consists missiles with low aspect ratio fins. In this paper, computational methods are used to predict normal force and center of pressure of missiles with very low aspect ratio fin configuration. A case study is selected for comparative analysis and optimization study. Computational Fluid Dynamics (CFD) results for the case study are compared with results obtained using theoretical and empirical methods at supersonic Mach numbers. In addition to total forces acting on the body-strake model, strake panel alone and body alone forces are obtained to calculate interference effects. The effects of strakes on flow field are analyzed by comparing body alone and body-strake pressure fields. The normal force and pitching moment of the strake unit are calculated by subtracting body alone values from body-strake results. The normal force and calculated center of pressure values of the strake unit (D57) are compared with data from LTV HSWT 655 Wind Tunnel Test Data [White, 1994]. The CFD results are robust and in agreement with the experimental results; however, for testing accuracy of theoretical methods, further research is required. After validating CFD tool, with the addition of fixed tail surfaces, a CFD based optimization study is performed to minimize coupling effects due to sideslip angle in the longitudinal maneuver plane and keep static margin constant.*

### INTRODUCTION

Very low aspect ratio fin configurations are mainly used for highly maneuverable supersonic missiles due to their compact structures and favorable aerodynamics at moderately high angles of attack. However, missiles with very low aspect ratio fins (also called as strakes) have non-linear aerodynamic characteristics and are difficult model using linear theories. There are vortex sheets attached along the long strake tip edges due to mutual interference of the flow fields of the body and the strake. Due to this phenomenon vortex lift is created. As a result, strakes are employed to increase the lift of the missiles and improve maneuverability [White, 1994]. Moreover, they are also used as cableways removing the need for extra fairings on the body. Historically, there exist theoretical and empirical methods employed for estimating the normal force and center of pressure of fins with very low aspect ratio. In this paper, a case study is selected for CFD analysis to estimate normal force and center of pressure of the strake unit, and the results obtained via CFD are compared with theoretical and empirical methods. After investigating the aerodynamic modelling methods for very low aspect ratio

---

<sup>1</sup> Aerodynamic Design Engineer at ROKETSAN Missile Industries Inc., Email: engin.usta@roketsan.com.tr

<sup>2</sup> Aerodynamic Design Engineer at ROKETSAN Missile Industries Inc., Email: kivanc.arslan@roketsan.com.tr

<sup>3</sup> Professor in Aerospace Engineering, Email: tuncer@ae.metu.edu.tr

missile fins, an optimization study is performed to reduce coupling effects on the pitching plane due to sideslip angle.

The methods included in this paper consist of the following:

- a.) White's Method
- b.) Missile DATCOM 2009 / Rosema's Method
- c.) Navier-Stokes Method

The flight conditions for aerodynamic analyses are as follows:

$$Mach = 2.01 \text{ and } \phi = 0^\circ, \phi = 45^\circ$$

$$\alpha = 0^\circ - 30^\circ$$

The model for this study is the (+) orientation four panel strake (D57)-body configuration shown below.

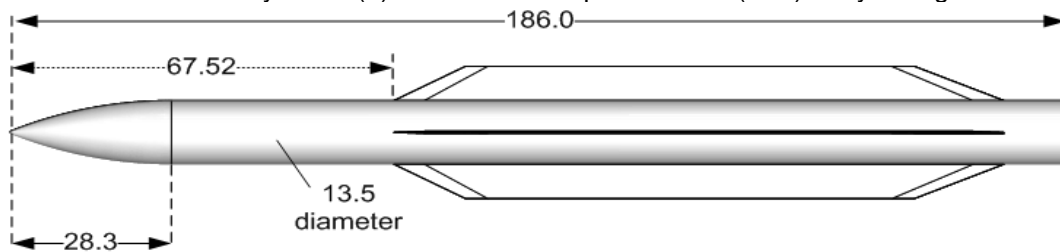


**Figure 1** Body Geometry and Strake Panel (D57) Placement for the Test Case Configuration [All dimensions are in inches]

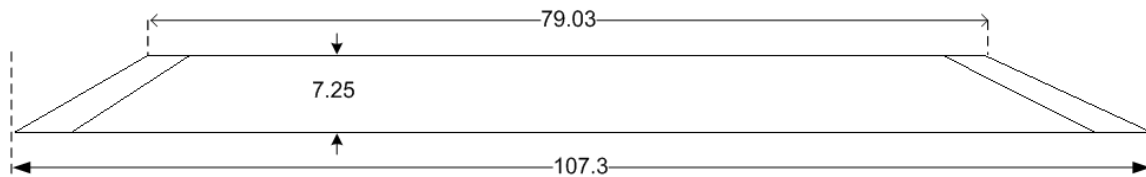


**Figure 2** Strake Panel (D57) Planform Geometry for the Test Case Configuration [All dimensions are in inches]

### METHOD

The surface meshes of the body-strake (D57) and body alone configurations together with volume meshes of the solution domains are represented in Figure 3. It must be noted that since no drag calculation is performed and only static aerodynamic coefficients are evaluated, it is not necessary to use very fine grids.

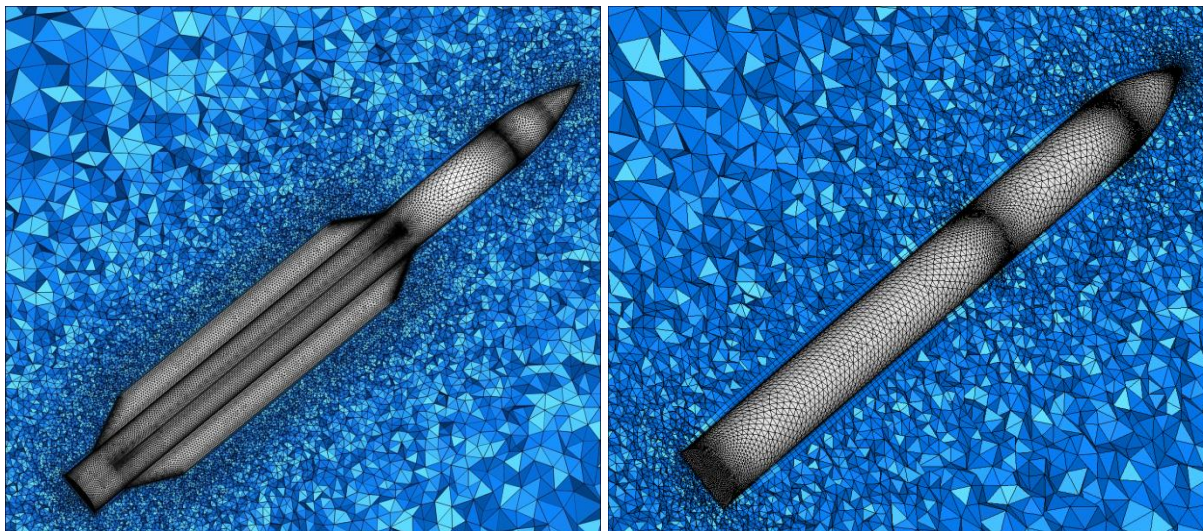


**Figure 3** Surface and Volume Mesh for the Body-Strake Configuration and Body Alone Solutions

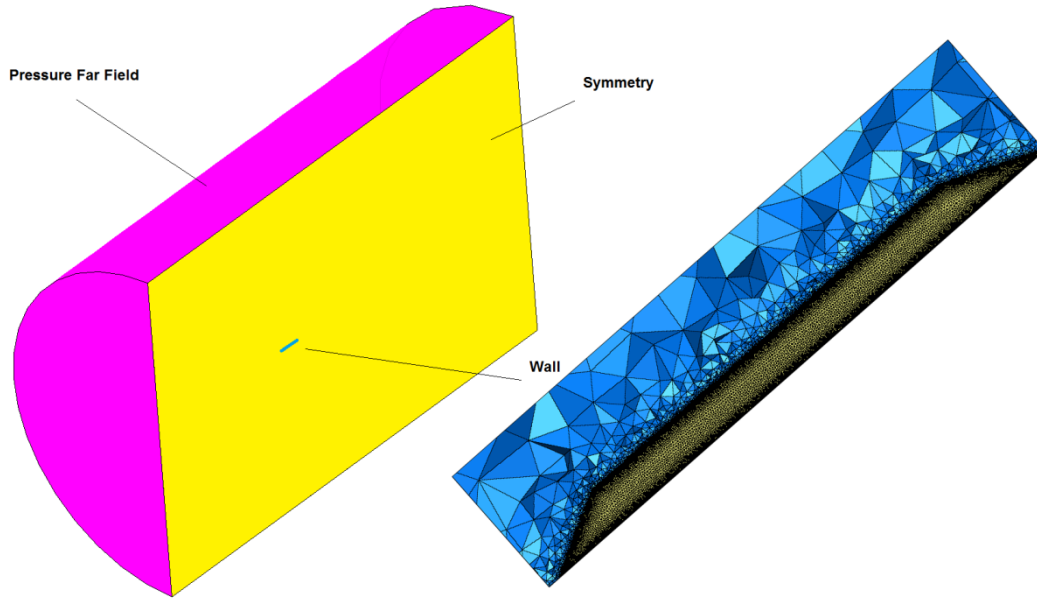


**Figure 4** Solution Domain and Surface Mesh for the Strake-Panel Alone Solution

The solution domain for strake alone calculations are presented in Figure 4. The strake panel alone solution is obtained using symmetry approach. Results for strake-set (four panels) are calculated by using summation of panel alone data for the panels in (+) orientation which are 2<sup>nd</sup> and 4<sup>th</sup> panels. The strake alone results are used to calculate the interference effects in the force breakdown study.

$$C_{N_{strake\ alone}} = C_{N_{panel\ 2}} + C_{N_{panel\ 4}}$$

For the calculation of the aerodynamic coefficients, reference length is taken as the missile body diameter and reference area is maximum frontal area of the cylindrical body cross section. Center of pressure of the strake unit is taken as the distance from leading edge location.

$$L_{ref} = 13.5\ in$$

$$S_{ref} = 143.1387\ in^2$$

The normal force and pitching moment of the strake unit are calculated by subtracting body alone values from body-strake values. Using the normal force and pitching moment of the strake unit the center of pressure of the strake unit is calculated.

$$C_{N_{strake-unit}} = C_{N_{body-strake}} - C_{N_{body-alone}}$$

$$C_{m_{strake-unit}} = C_{m_{body-strake}} - C_{m_{body-alone}}$$

$$X_{CP_{strake-unit}} = \frac{C_{m_{strake-unit}}}{C_{N_{strake-unit}}}$$

ANSYS Fluent is used as CFD solver. Three dimensional, compressible, steady, Reynolds-Averaged Navier-Stokes equations were solved by using finite volume method to calculate flow field around the missile and k- $\epsilon$  turbulence model is used to model viscous effects.

The pressure field around the body-strake and body alone configurations for D57 strake are shown below in Figure 5 . From the slices shown in Figure 5, it can be observed that as the distance along the strake increases from leading edge, the pressure difference between upper and lower surfaces increases.

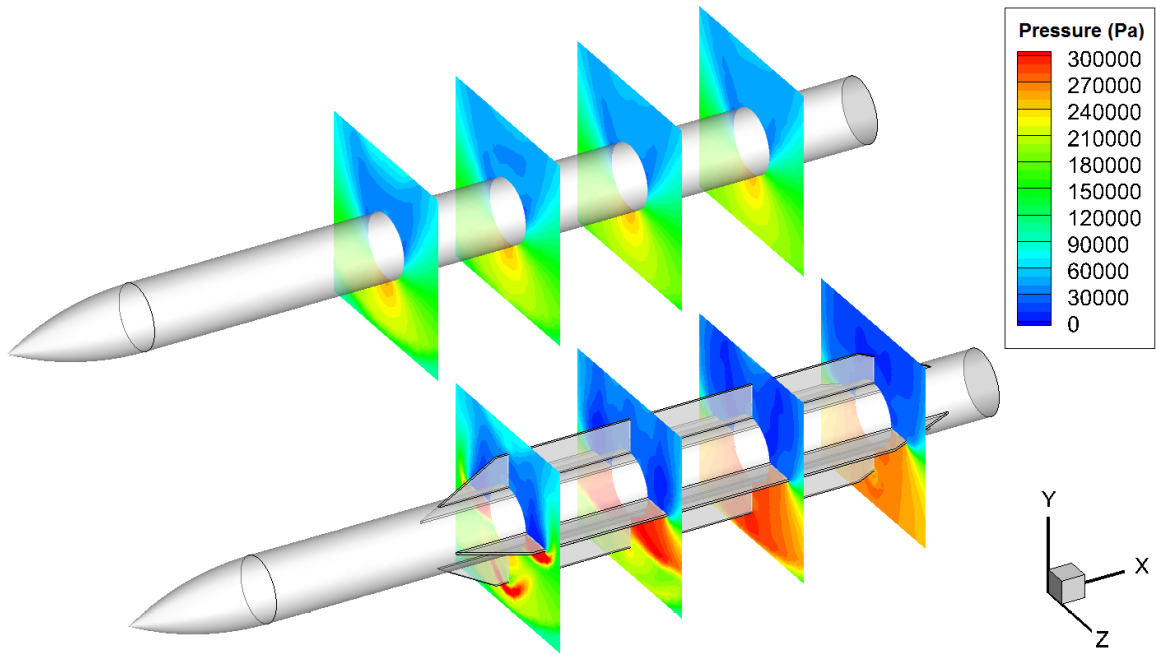


**Figure 5** The Pressure Contours at Slices Along the (D57) Strake-Body and Body Alone Configuration

Aerodynamic coefficients of D57 are also predicted using engineering level fast prediction tools.

In older versions of Missile DATCOM, Lucero’s method with no special treatment was employed for missiles with strakes [Lucero, 1984]. In Missile Datcom 2009, strakes are categorized into three parts and different methods are employed for each case. These categories consist of rectangular, delta, and trapezoidal fins. For rectangular fins Lucero’s empirical method improved by Rosema is employed whereas for delta fins linear theory with thickness correction factors is used. For trapezoidal fins there is a transition from Lucero’s method to linear theory [Auman, Doyle, 2008].

In White’s method, an empirical correlation is developed between geometrical parameters with normal force and center of pressure by using a wide range of wind tunnel database. The geometrical parameters consist of the strake span, body radius, body maximum frontal area and strake planform area for normal force estimation of the strake unit.

Results obtained for strake unit using Navier-Stokes, Missile DATCOM 2009, White’s Method and wind tunnel experiment are presented in Figure 5 and Figure 6 at Mach number 2.01 and  $\phi=0^\circ, 45^\circ$ .

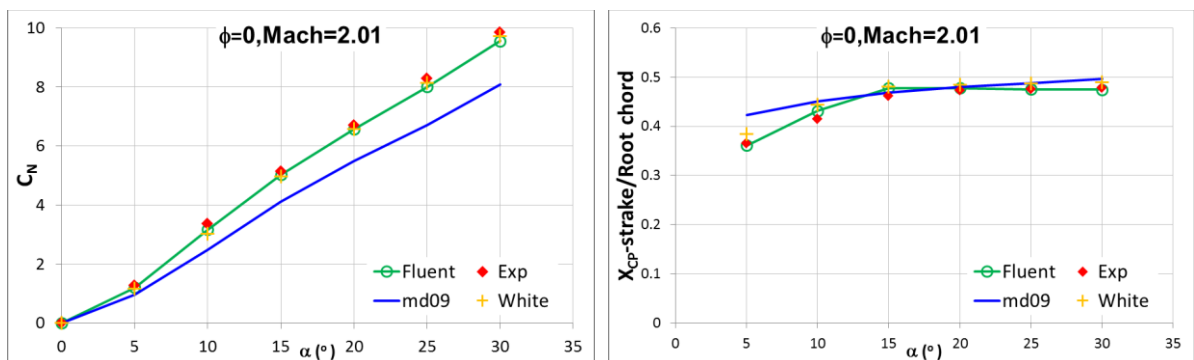


**Figure 6** Comparison of the Experimental Normal Force and Center of Pressure of the Strake Unit (D57) with Predicted Values (Mach=2.01,  $\phi=0$ )

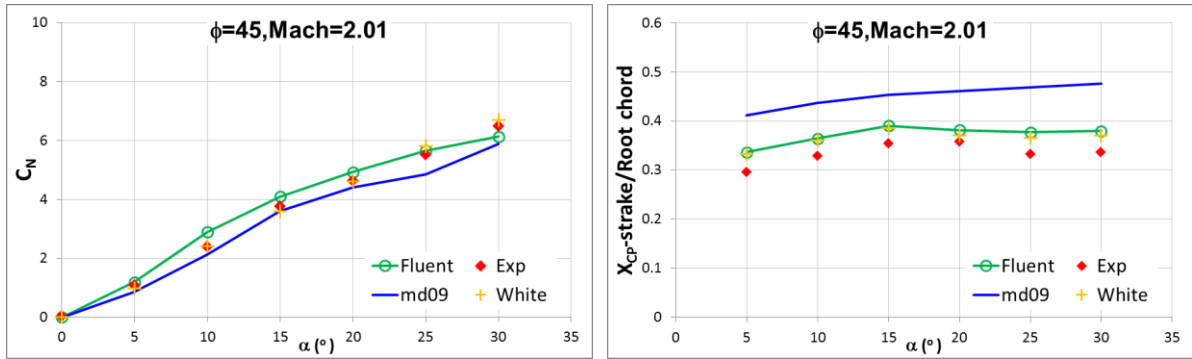


**Figure 7** Comparison of the Experimental Normal Force and Center of Pressure of the Strake Unit (D57) with Predicted Values (Mach=2.01,  $\phi=45$ )

The results are shown above. According to the figures it can be concluded that, White’s method and Reynolds-Averaged Navier Stokes method are very good for estimating the normal force and center of pressure of the strake unit for this configuration. Although there is improvement in Missile DATCOM version 2009, still it is not accurate enough and does not have the robustness of the White’s method and Navier-Stokes method.

A force breakdown is performed at Mach 2.01 using the body alone, strake alone and body-strake CFD solutions. In the body-strake CFD solutions, zonal forces of the body and strake which are body in the presence of the strake and strake in the presence of the body are also output. Force increment of the body is found by subtracting body alone data from body in the presence of strake data, meanwhile, force increment of the strake is calculated by subtracting strake alone data from the strake in the presence of body values. The results are shown in the figure below.

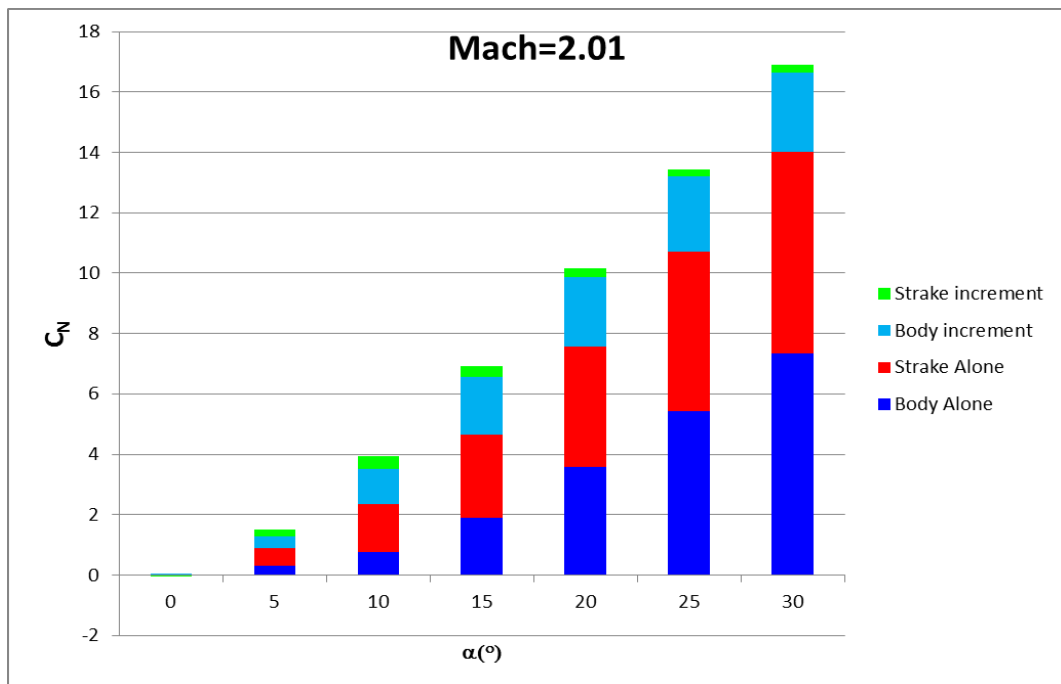


**Figure 8** The Breakdown of the Interference and Component Normal Forces

According to the results, the body and strake alone normal forces form up the main part of the total normal force produced. Moreover, body incremental force due to interference with strake is quite important compared to the strake incremental force for this body-strake configuration and its amount gets higher as the angle of attack increases.

**OPTIMIZATION STUDIES**

**Testing of the Optimization Tool Used for Design Studies**

A stochastic optimization method namely the Particle Swarm Optimization (PSO) is employed for design optimization study. In this part, testing of this optimization method on a test function is presented. The flowchart for PSO algorithm is presented in Figure 9.

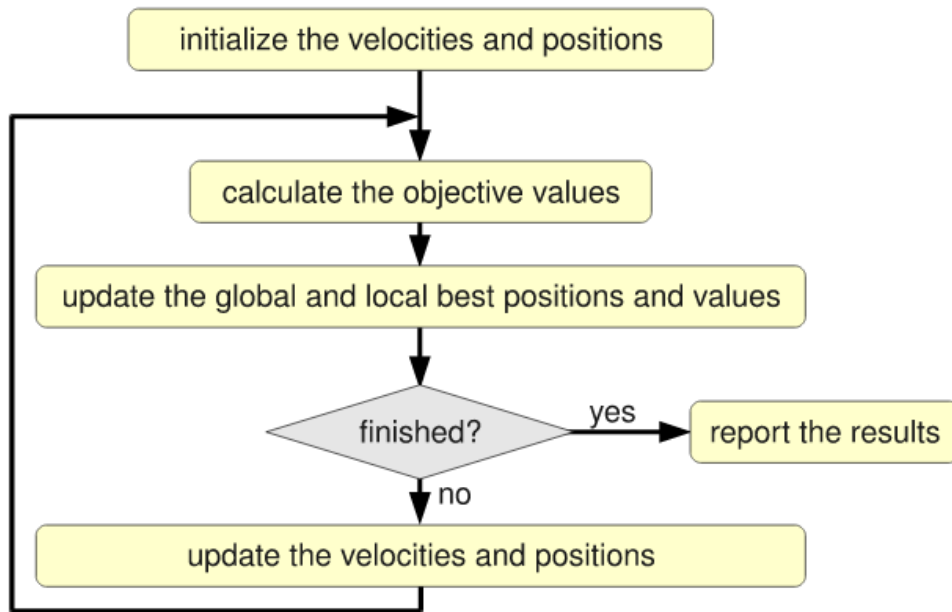


**Figure 9** The Flowchart of the PSO algorithm [Schoene, 2011]

The details of the PSO method can be found in Mishra’s paper [Mishra,2006]. Before aerodynamic performance optimization, a preliminary optimization study of the test function “Eggholder” is made by using PSO optimization method, and the results are shown below.

$$f(x, y) = -(y + 47) \cdot \sin\left(\sqrt{\left|y + \frac{x}{2} + 47\right|}\right) - x \cdot \sin\left(\sqrt{|x - (y + 47)|}\right) \quad (\text{Eggholder Function})$$

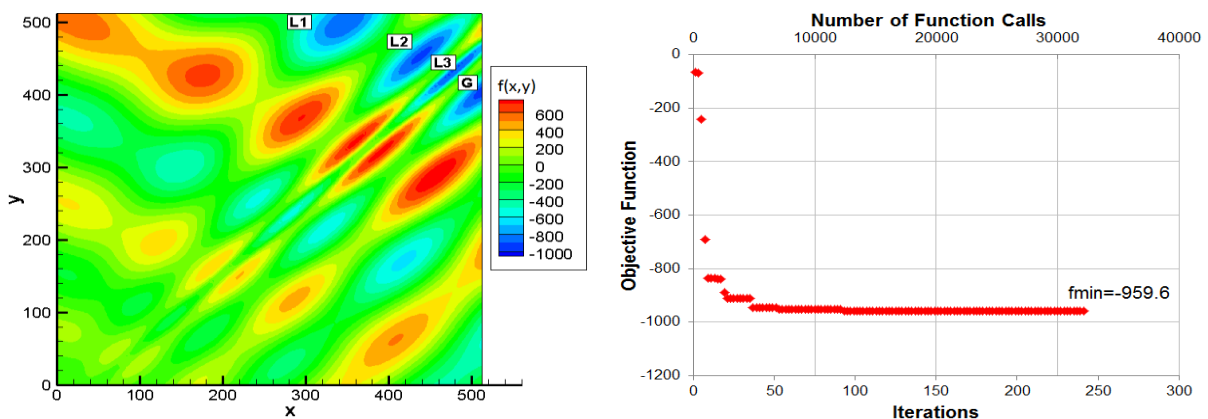


**Figure 10** Contour Plot of “Eggholder” Function & Number of Iterations and Number of Function Calls During Iterations by Particle Swarm Optimization Method (PSO)

The local minimas shown by L1, L2 and L3 above in the contour plot are:

$$f(347.3, 499.4) = -888.9$$

$$f(439.5, 454.0) = -935.3$$

$$f(482.3, 432.9) = -956.9$$

and the global minimum shown by "G" above in the contour is:

$$f(512.0, 404.2) = -959.6$$

It can be observed that PSO method ensures global solution and can be used for aerodynamic performance optimization.

### Optimization Problem Definition

The main aim of the CFD based optimization study is to reduce the coupling effects due to sideslip angle from the longitudinal maneuver plane. Meanwhile, it is aimed to keep static margin in the range of 1-1.2. For these aims the performance parameters of the configurations are evaluated by meshing them automatically in GAMBIT and solving by using ANSYS FLUENT solver. The three changing geometrical parameters during optimization iterations are leading edge location, chord length and span length of the strake unit as shown in the figure below. The tail surfaces are added to the initial body geometry and tail geometry is kept constant. The sweep angles at the leading and trailing edges of the strake planform are kept constant.

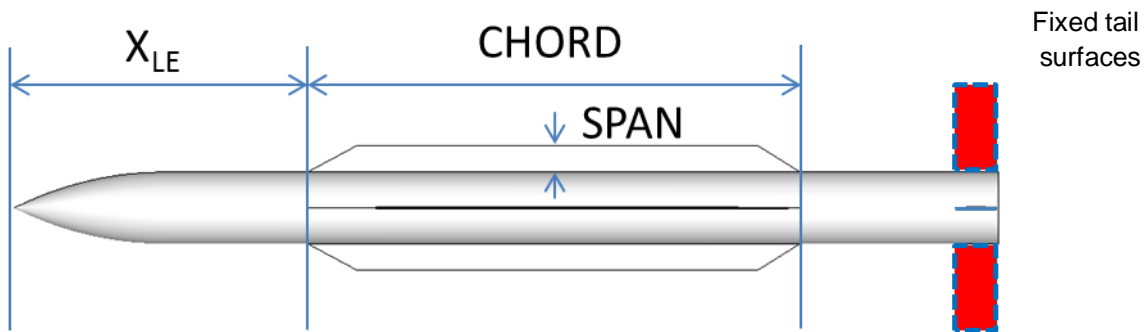


**Figure 11** Geometric Parameters of the Optimization Problem

The limits imposed on the geometrical parameters related to the strakes are given in the table below:

**Table 1** The Limits Of Geometrical Parameters

Geometric Parameter	Minimum (in)	Maximum (in)
Chord	27.6	107
Span	2.36	7.87
Leading edge from nose	29.5	108.3

The pitching moments are calculated with respect to the nose. The static margin is calculated with respect to the center of gravity location given below. Reference length is taken as the missile diameter and reference area is taken as the area of the cross section:

$$L_{ref} = 13.5 \text{ in}$$

$$S_{ref} = 143.1387 \text{ in}^2$$

$$X_{CG} = 93 \text{ in}$$

The target aerodynamic performance parameters are tabulated below. As stated below the static margin must be in between 1.0 and 1.2. The pitching moment differential for Mach 2.01 between

sideslip angles of 5 and 10 degrees is to be minimized. The flight conditions in which CFD solutions obtained for each configuration are:

$$Mach = 2.01$$

$$\alpha = 8^\circ$$

$$\beta = 5^\circ, 10^\circ$$

**Table 2** Target Aerodynamic Performance Parameters at Mach 2.01

Performance Parameter	Target
Static Margin at $\alpha=8^\circ$ , $\beta=10^\circ$	Keep between 1.0 and 1.2
$ C_m(\beta = 10^\circ) - C_m(\beta = 5^\circ) $ , $\alpha = 8^\circ$	Minimize

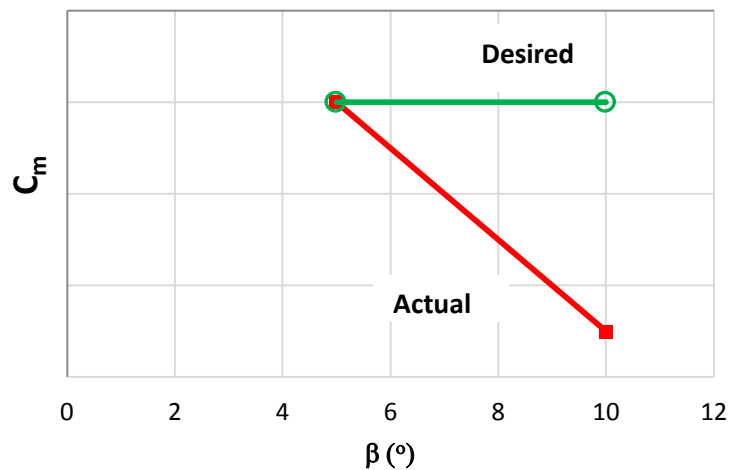


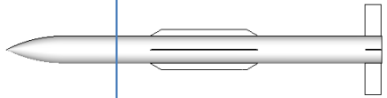
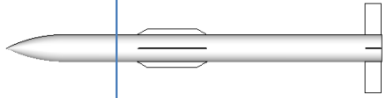
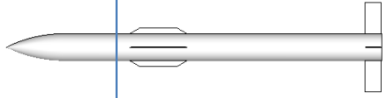
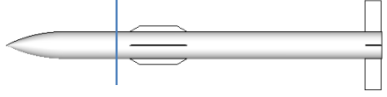
**Figure 12** The Desired and Real Pitching Moment Curves with Sideslip Angles at 5 And 10 Degrees Sideslip Angle

The target aerodynamic performance parameters given in Table 2 are converted into the objective function to be minimized in the optimization problem. The first part of the objective function is based on minimizing the pitching moment differential with changing side slip angle. This is illustrated in Figure 12 and as can be seen it is aimed to flatten  $C_m$ - $\beta$  curve. The second part is for keeping the static margin in a certain range as a controlling parameter.

## RESULTS

The PSO optimization iterations continued for 67 steps. The change of the geometry of best member of the population during iterations is given in the following table.

**Table 3** The Change of the Strake Planform Geometry and Placement on the Body During Optimization Steps

Iteration Number	Missile Configuration Geometry
1 (Baseline)	
10	
20	
30	
67 (Optimum)	

As can be observed from the Table 3, the leading edge location swings back and forth. The chord length and span length decreases continuously during the iterations, approaching lower limits in the final iterations. Principally, the aim to reduce coupling effect on the pitching moment make the strake planform get smaller during iterations. It must be emphasized that the strake unit must not vanish since it is essential for satisfying the static margin requirement.

The change of the objective function corresponding to the best member of the population at each iteration step during optimization iterations is presented in Figure 13.

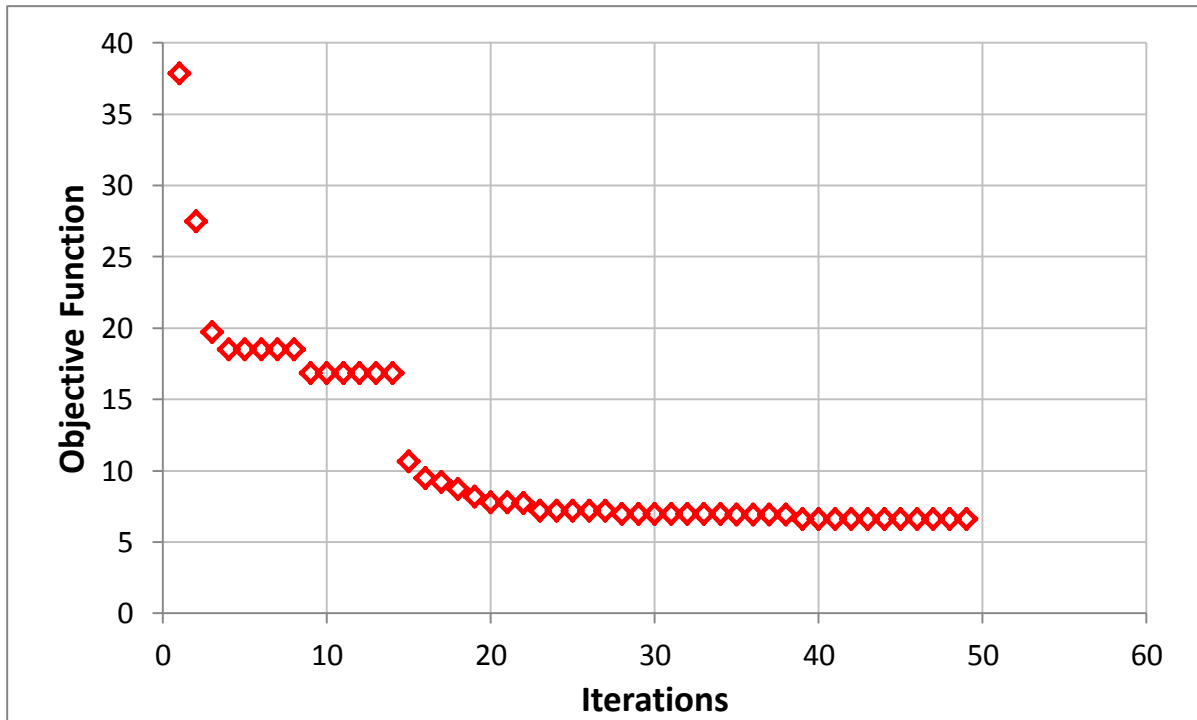


**Figure 13** The Change of the Objective Function During Optimization Iterations

The final optimum geometry details are given in Table 4. As can be seen from the table, chord and span length decrease continuously.

**Table 4** The Comparison of the Geometric Parameters of The Baseline and Optimum Solutions

	<b>Chord Length</b>	<b>Span Length</b>	<b>Leading Edge Location</b>
<b>Baseline</b>	93.1	4.97	55.38
<b>Optimum (PSO)</b>	27.9	2.65	57.6

**Table 5** The Comparison of the Aerodynamic Performance of the Baseline and Optimum Solutions

	<b><math>\Delta CM</math></b>	<b>Static Margin [d]</b>
<b>Baseline</b>	7.48	0.64
<b>Optimum (PSO)</b>	2.57	1.13

From Table 5, the substantial decrease in pitching moment differential can be observed. The static margin is successfully kept in the range between 1.0 and 1.2.

The optimum missile configuration obtained at the end of the iterations is shown below:

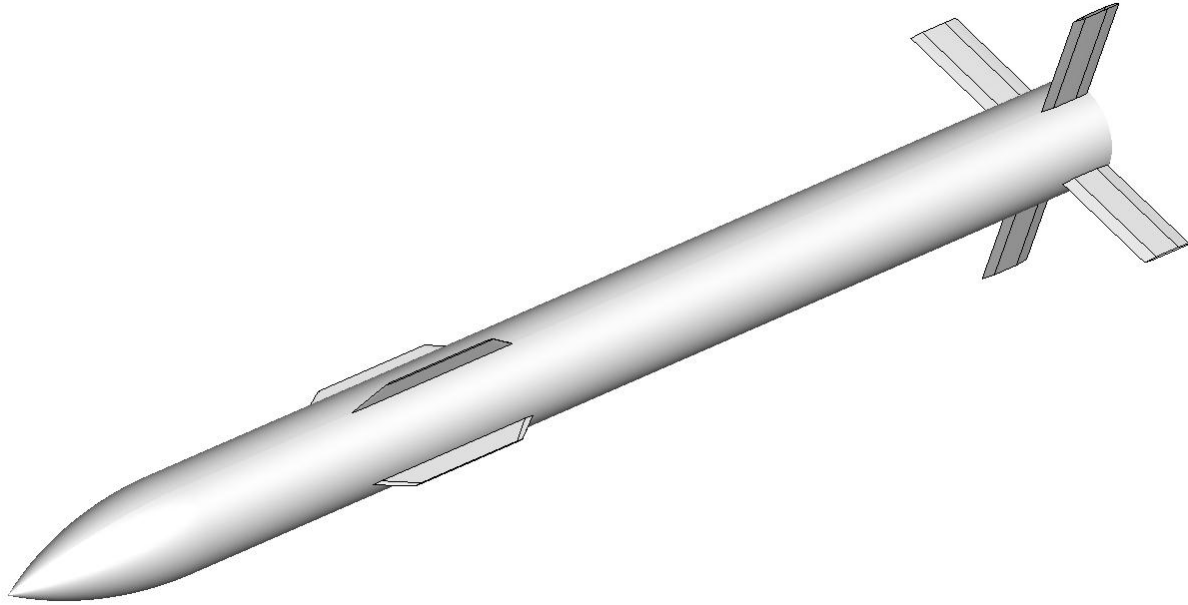


**Figure 14** Optimum Missile Strake Geometry (Isometric View)

The pitching moment curve with sideslip angle is given below:

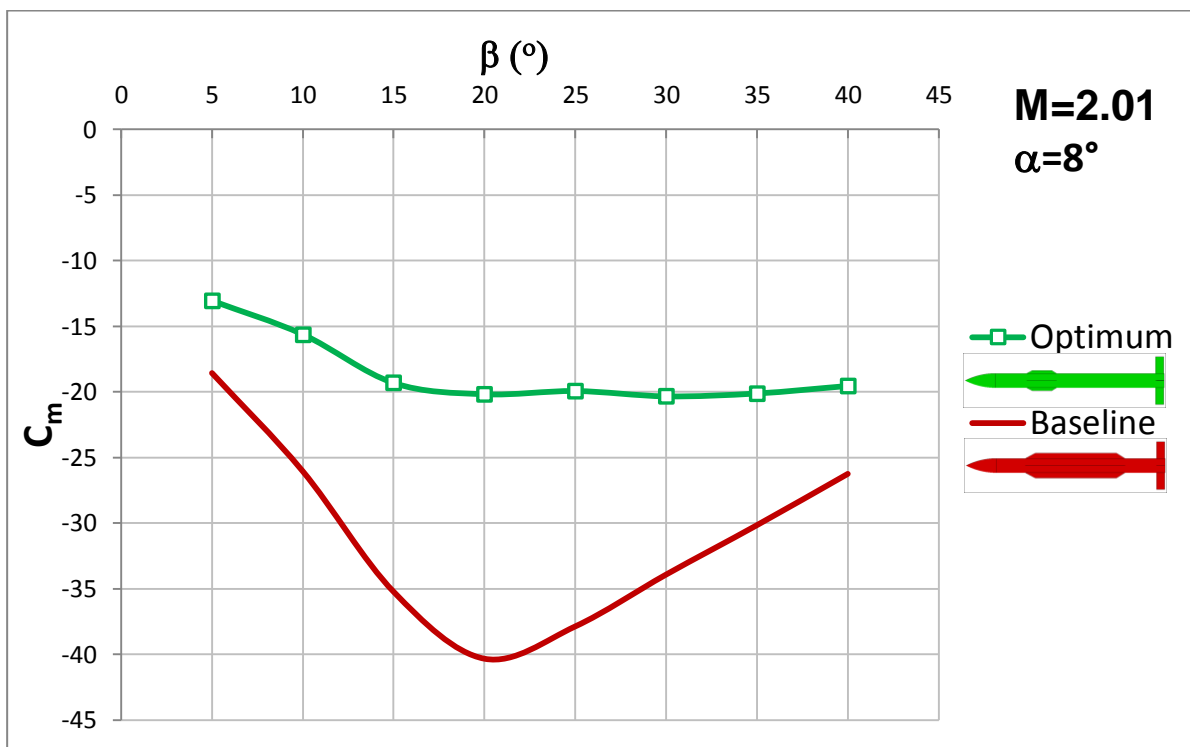


**Figure 15** The Change of The Pitching Moment Coefficient with Sideslip Angle For The Optimum and Baseline Missile Configurations

From Figure 15 it can be seen that pitching moment dependency on sideslip angle is minimized successfully and pitching moment curve with sideslip angle is flattened.

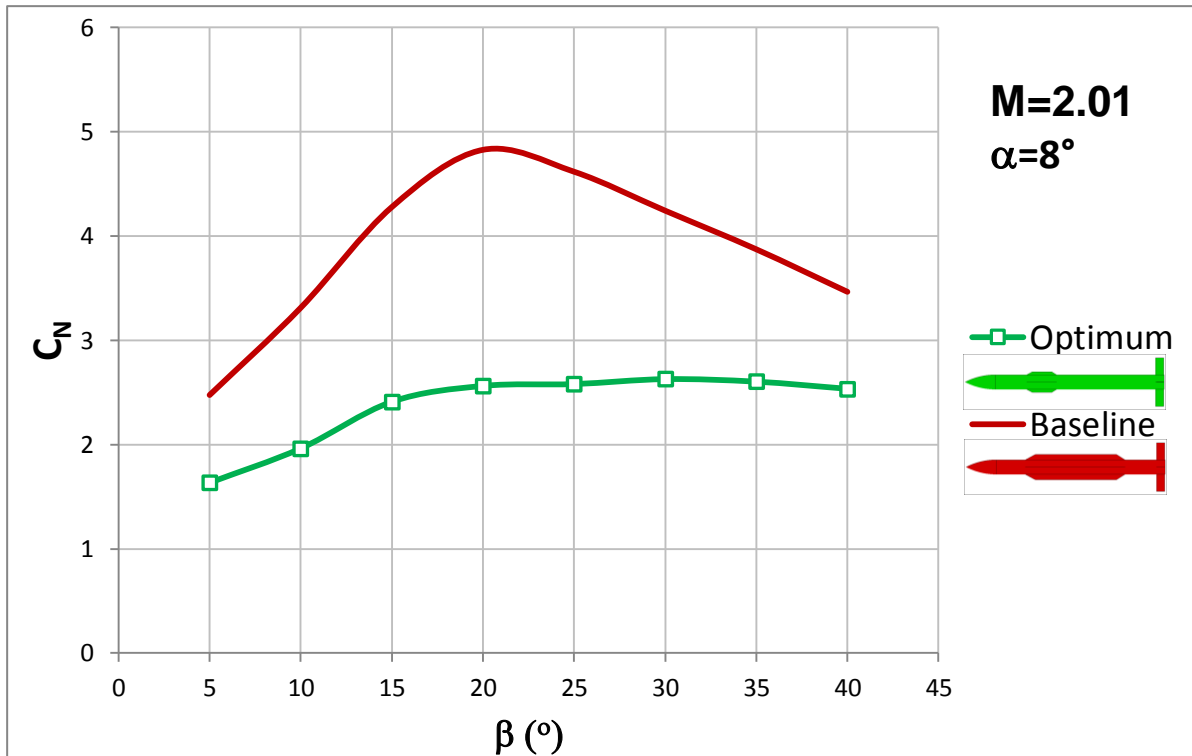


**Figure 16** The Change of the Normal Force Coefficient with Sideslip Angle for the Optimum and Baseline Missile Configurations

The static margin at 10 degrees sideslip angle is in the desired range. Although there is no term related to the normal force in the objective function of the optimization study, its coupling from sideslip angle is also reduced as illustrated in Figure 16.

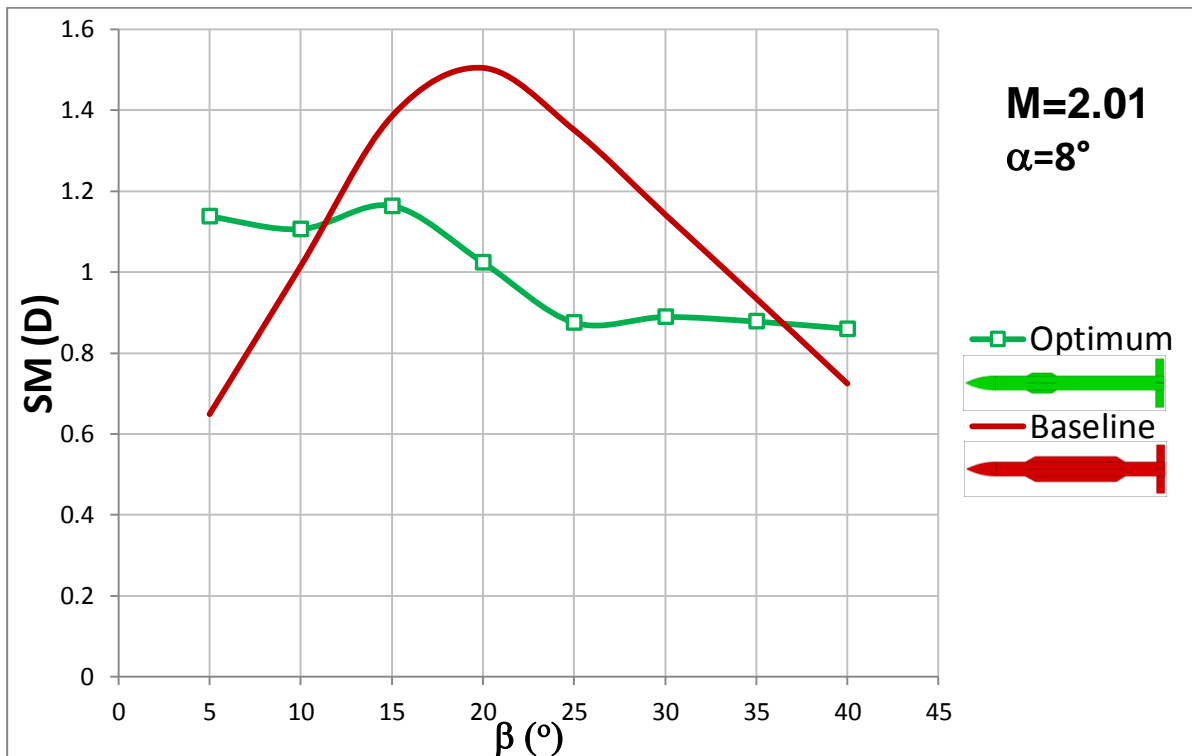


**Figure 17** The Change of the Static Margin with Sideslip Angle for The Optimum and Baseline Missile Configurations

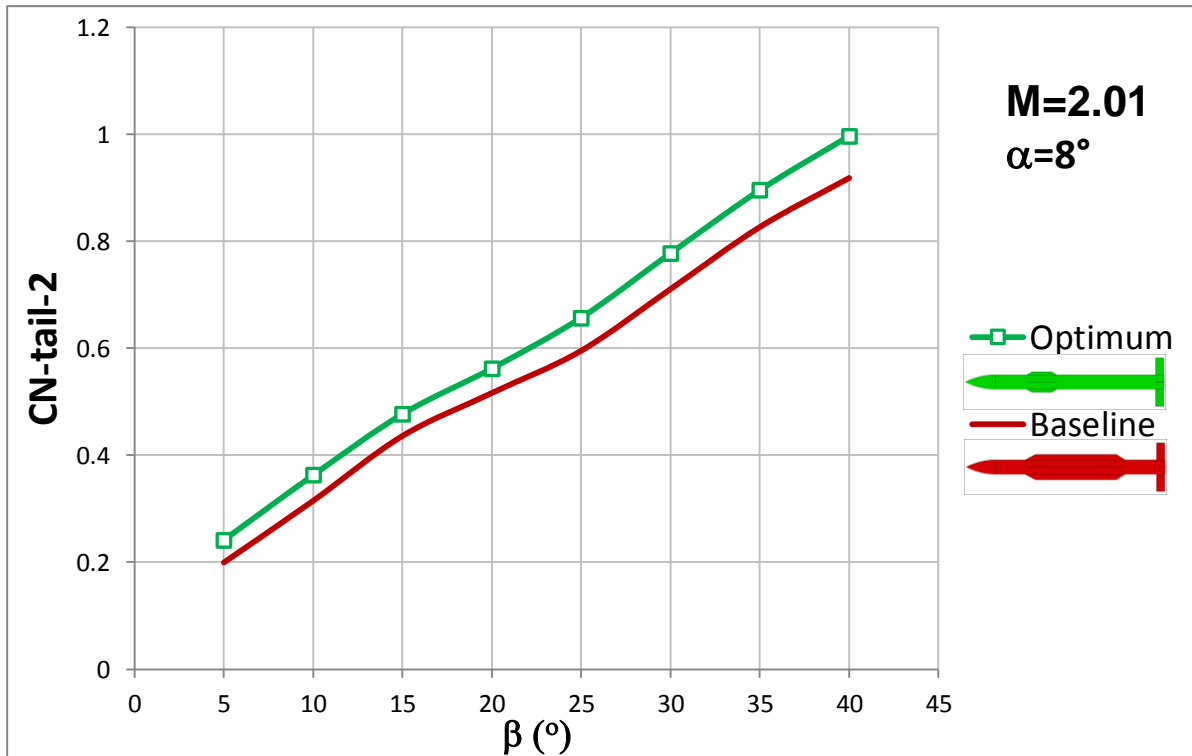


**Figure 18** The Change of The Panel Normal Force of The Tail with Sideslip Angle for The Optimum and Baseline Missile Configurations

The streamlines of the asymmetric flow developed over the optimum and baseline missiles are shown in Figure 19 and Figure 20 respectively.

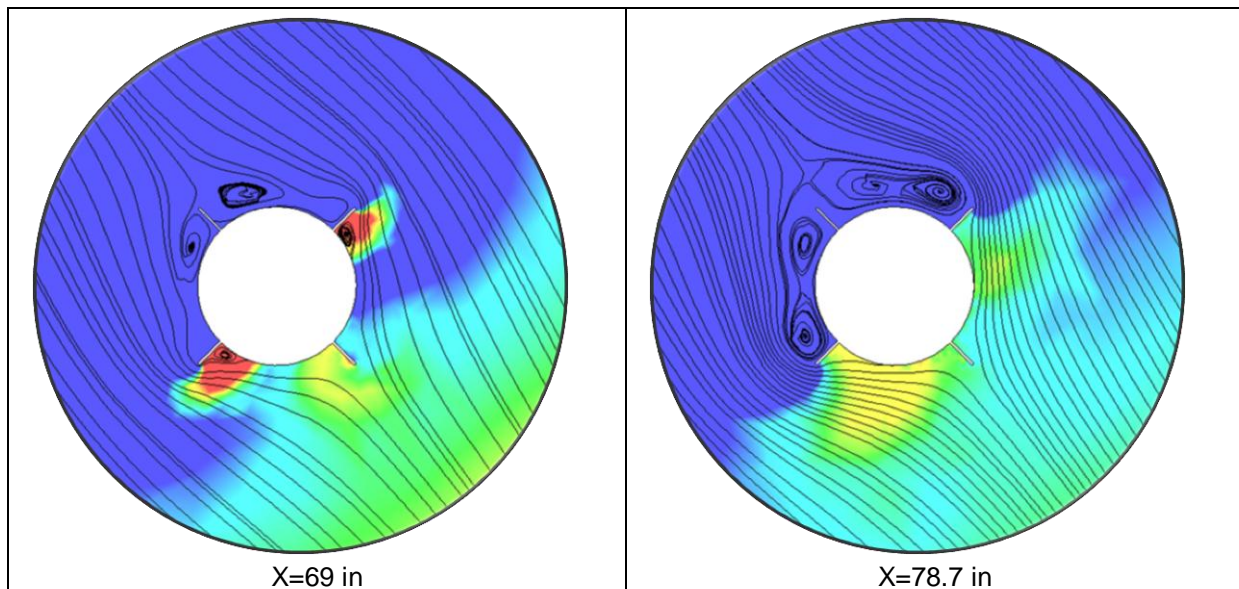


**Figure 19** The Streamlines at Slices Along the X Axis for The Optimum Missile

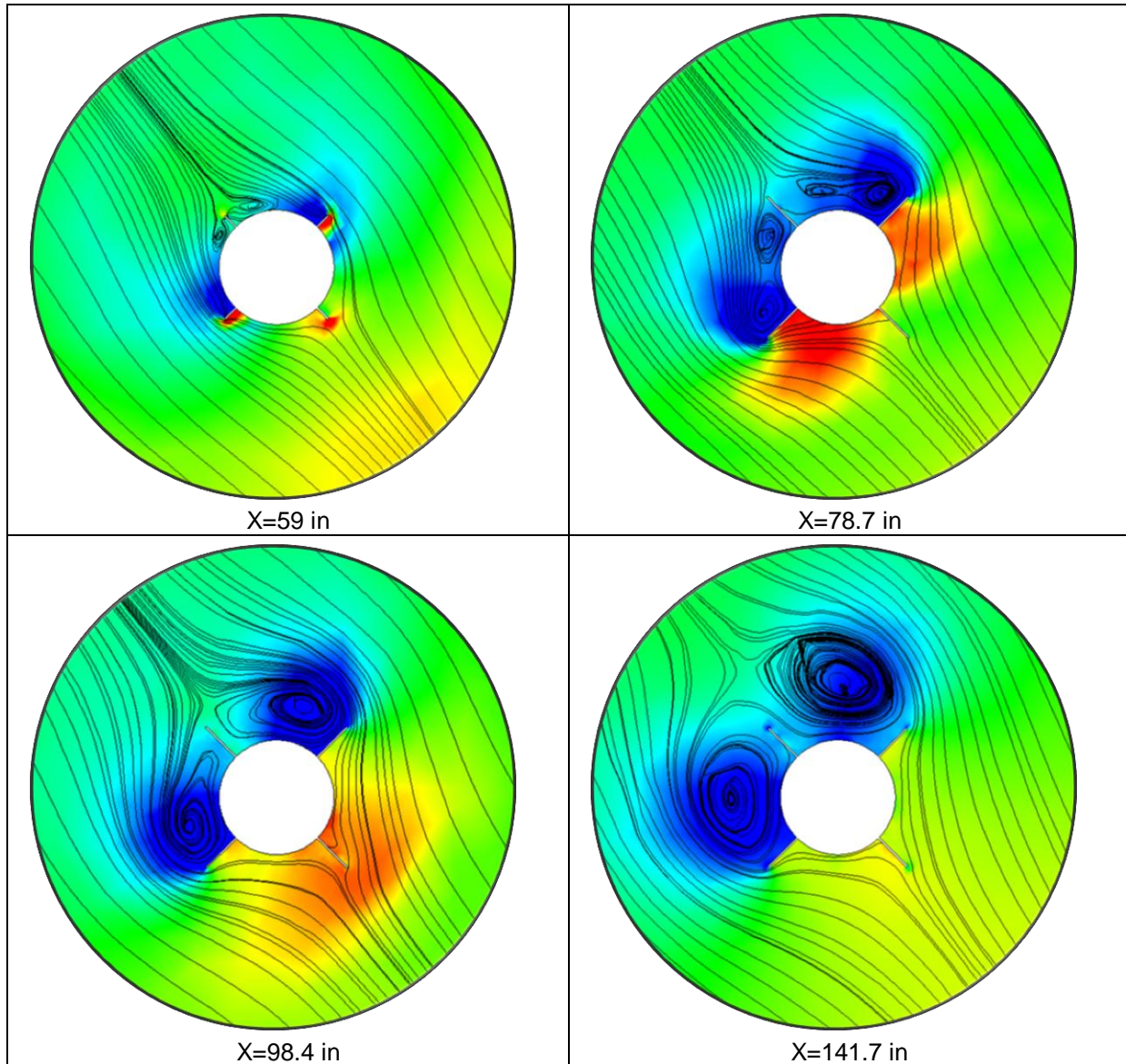


**Figure 20** The Streamlines at Slices Along the X Axis for the Baseline Missile

Comparing the streamlines of the optimum and baseline configurations, it can be seen that two vortices develop in the upper flow region close to the leading edge location. Further moving along the chord, only a single concentrated vortex remains in the region.

### CONCLUSION

- In the first part, CFD and engineering level fast prediction tools were used to predict the aerodynamic characteristics of the body-strake configuration D57 at supersonic flow conditions. Calculated results were compared with existing experimental values.
- Interference effects of body-strake on aerodynamic coefficients were investigated.
- For the estimation of the normal force and center of pressure of the D57 strake configuration, White's method and Navier-Stokes methods produced accurate results. Although improvement is made in DATCOM 2007 and newer versions, it still needs improvement for estimating the center of pressure and normal force of the strake unit in this study. The White's method needs to be further investigated since the test case was taken from his study. On the

other hand, CFD is robust and applicable for different cases as proved in test case study and also mentioned in literature. [White, 1994].

- As the chord length of the strake increases, the pressure difference between upper and lower surfaces of the strake unit increases. The pressure at upper surfaces becomes more negative and the pressure at lower surfaces becomes more positive along the chord.
- The difference between body in the presence of the strake unit and body alone (body interference due to strake) normal force, is large compared to the strake in the presence of the body and strake alone difference. This implies that the vortices shed on the body along the root chord of the strake unit increase the body normal force.
- Using CFD based prediction methodology; an optimization study of aerodynamic performance parameters for the test case missile configuration with strakes and tail surfaces was performed.
- From optimization study, it was discovered that the pitching moment coupling could be reduced significantly by placing small strake surfaces at appropriate location on the body in addition to the tail surfaces while satisfying certain static margin requirement.

## References

*Ansys Fluent Users Guide Release 15.0*, Fluent Inc., November 2013

Auman, L., Doyle, J., Rosema, C., and Underwood M. (Aug. 2008) *MISSILE DATCOM User's Manual - 2008 Revision*, U.S. Army Aviation & Missile Research, Development and Engineering Center,

Lucero, E. F. (Jan. 1984) *Empirical Curves for Predicting Supersonic Aerodynamics of Very Low Aspect Ratio Lifting Surfaces*, American Institute of Aeronautics and Astronautics, 22nd Aerospace Sciences Meeting, AIAA Paper 84-0575

Mishra, S.K., (2006) *Global Optimization by Differential Evolution and Particle Swarm Methods: Evaluation on Some Benchmark Functions*, Social Science Research Network (SSRN) , Working Papers Series, retrieved from <http://ssrn.com/abstract=933827>

Rosema, C., Underwood, M., and Auman, L. (Jun. 2007) *Recent Fin Related Improvement for Missile DATCOM*, American Institute of Aeronautics and Astronautics, 25th Applied Aerodynamics Conference, AIAA 2007-3937

Schoene, T. (2011) *Step-Optimized Particle Swarm Optimization*, (Master's thesis, College of Graduate Studies and Research), retrieved from [http://www.cs.usask.ca/~spiteri/students/tschoene\\_msc\\_thesis.pdf](http://www.cs.usask.ca/~spiteri/students/tschoene_msc_thesis.pdf)

Sharpes, D. G. (1985) *Validation of USAF Stability and Control DATCOM*, Air Force Wright Aeronautical Laboratories, AFWAL-TR-84-3084

White, J. T. (Aug. 1994) *A Method for Predicting Combined Dorsal Normal Force and Center-of-Pressure Location at Supersonic Mach Numbers*, American Institute of Aeronautics and Astronautics, 19<sup>th</sup> Atmospheric Flight Mechanics Conference, AIAA-94-3466-CP